The *PRA1* Gene Family in Arabidopsis[1][W]

Claire Lessa Alvim Kamei, Joanna Boruc, Klaas Vandepoele, Hilde Van den Daele, Sara Maes, Eugenia Russinova, Dirk Inzé*, and Lieven De Veylder

Instituto de Bioquímica Médica, Universidade Federal do Rio de Janeiro, Rio de Janeiro, RJ 21941–590, Brazil (C.L.A.K.); and Department of Plant Systems Biology, Flanders Institute for Biotechnology (C.L.A.K., J.B., K.V., H.V.d.D., S.M., E.R., D.I., L.D.V.), and Department of Molecular Genetics, Ghent University, B–9052 Gent, Belgium (C.L.A.K., J.B., K.V., H.V.d.D., S.M., E.R., D.I., L.D.V.)

Prenylated Rab acceptor 1 (PRA1) domain proteins are small transmembrane proteins that regulate vesicle trafficking as receptors of Rab GTPases and the vacuolar soluble *N*-ethylmaleimide-sensitive factor attachment receptor protein VAMP2. However, little is known about PRA1 family members in plants. Sequence analysis revealed that higher plants, compared with animals and primitive plants, possess an expanded family of PRA1 domain-containing proteins. The Arabidopsis (*Arabidopsis thaliana*) PRA1 (AtPRA1) proteins were found to homodimerize and heterodimerize in a manner corresponding to their phylogenetic distribution. Different *AtPRA1* family members displayed distinct expression patterns, with a preference for vascular cells and expanding or developing tissues. *AtPRA1* genes were significantly coexpressed with Rab GTPases and genes encoding vesicle transport proteins, suggesting an involvement in the vesicle trafficking process similar to that of their animal counterparts. Correspondingly, AtPRA1 proteins were localized in the endoplasmic reticulum, Golgi apparatus, and endosomes/prevacuolar compartments, hinting at a function in both secretory and endocytic intracellular trafficking pathways. Taken together, our data reveal a high functional diversity of AtPRA1 proteins, probably dealing with the various demands of the complex trafficking system.

Vesicle trafficking is a finely orchestrated process that allows nascent proteins to be transported throughout the cell. Vesicles travel between different compartments of the endomembrane system. The major components of this system comprise the endoplasmic reticulum (ER), the Golgi apparatus, vacuoles, and the plasma membrane. The ER is arranged as an intricate web of tubules and sheets in the cytoplasm. Along its surface, many proteins are synthesized, processed, and folded, some of which are incorporated into or exported to the Golgi apparatus through vesicle transport (Hanton et al., 2006). From the Golgi apparatus, vesicles carry materials to the lytic or storage vacuoles or simply secrete their contents at the plasma membrane. In contrast, through endocytosis, molecules and recycled membrane are internalized and sorted by vesicles to different types of endosomes (for reviews, see Geldner, 2004; Jürgens, 2004; Derby and Gleeson, 2007; Müller et al., 2007). The balance between arriving and departing vesicles, together with the characteristics of their contents, indicate the adaptation of cells to their surroundings. To control this process, several proteins are recruited and elaborated pathways are executed. Although conserved in eukaryotes, many key players of the vesicle transport machinery are still poorly described in plants.

Among the proteins involved in vesicle transport, small GTPases are of great importance (for review, see Molendijk et al., 2004). The Ras superfamily of small GTPases has been referred to as ''molecular switches,'' because of its cycling from a GTP-bound active state to a GDP-bound inactive state. In this ''on'' and ''off'' behavior, small GTPases are able to control a wide variety of cellular processes (Bourne et al., 1990). The largest branch of the superfamily consists of Rab GTPases (Rabs) that regulate vesicle trafficking (Segev, 2001). To function properly, Rabs must be inserted into cellular membranes and subsequently activated (for review, see Pfeffer and Aivazian, 2004). The association of Rabs with membranes requires a posttranscriptional modification at their carboxyl region by prenylation. While present in the cytosol, prenylated Rabs are kept in their inactive state, bound to the GDP dissociation inhibitor (GDI). The GDI masks the isoprenyl anchor of prenylated Rabs, avoiding membrane attachment. To catalyze the dissociation from the GDI, a GDI displacement factor (GDF) sequesters Rabs and ensures their retention in the membrane by restraining the action of the GDI. Once into the membranes, Rabs are finally activated by guanine exchange factors.

[1] This work was supported by grants from the Interuniversity Poles of Attraction Programme-Belgian Science Policy (P6/33), Conselho Nacional de Desenvolvimento Científico e Tecnológico (predoctoral fellowship to C.L.A.K.), European Union-Human Resources and Mobility for an Early Stage Training (grant no. MEST–CT–2004–514632 to J.B.), and Research Foundation-Flanders (postdoctoral fellowships to K.V. and L.D.V.).

* Corresponding author; e-mail dirk.inze@psb.ugent.be.

The author responsible for distribution of materials integral to the findings presented in this article in accordance with the policy described in the Instructions for Authors (www.plantphysiol.org) is: Lieven De Veylder (lieven.deveylder@psb.ugent.be).

[W] The online version of this article contains Web-only data.
www.plantphysiol.org/cgi/doi/10.1104/pp.108.122226

Rabs specifically localize within the cell, but how this specificity is obtained remains elusive. GDFs seem to fulfill this role, recruiting and providing specificity on membrane association. Since the identification of GDF activity (Soldati et al., 1994; Ullrich et al., 1994), only a small subset of proteins have been proposed with a GDF function. Prenylated Rab acceptor 1 (PRA1) was the first described protein with such a function (Sivars et al., 2003). PRA1s are small transmembrane proteins omnipresent in different vesicle trafficking events and interact with various kinds of proteins. In chemical synapses, PRA1 associates with Piccolo, a zinc finger protein of the presynaptic cytoskeletal matrix, suggesting a function in synaptic vesicle trafficking (Fenster et al., 2000). PRA1 also interacts with other prenylated small GTPases, such as the mouse Ha-Ras, N-Ras, TC21, and RhoA, as well as with the v-SNARE protein VAMP2 (Martincic et al., 1997; Figueroa et al., 2001), and it plays a role as modulator of the neural Glu transporter excitatory amino acid carrier 1 (Akiduki et al., 2007). Because of its capacity to interact with GTPases and SNARE proteins, PRA1 might connect these two large groups of proteins to efficiently control vesicle docking and fusion events.

In plants, a PRA1-related protein had been reported as an interactor of the cauliflower mosaic virus (CaMV) movement protein (Huang et al., 2001). Here, we functionally characterized the Arabidopsis (*Arabidopsis thaliana*) *PRA1* gene family. In our analysis, 19 proteins, designated AtPRA1, were found to contain the PRA1 motif. The different family members formed homodimers and heterodimers. In 8-d-old seedlings, *AtPRA1* genes were expressed in vascular, expanding, or developing tissues. The presence of Rabs in a set of coexpressed genes with different *AtPRA1* genes, and their Gene Ontology (GO) profiles, suggested a conserved function of AtPRA1 in vesicle trafficking. This hypothesis was confirmed by the subcellular localization of different AtPRA1 proteins in the Golgi apparatus, ER, and endosomal compartments. Based on our results, we propose a role for PRA1 proteins in the control of vesicle transport between different intracellular compartments of plant cells.

RESULTS

The *AtPRA1* Family Comprises 19 Members

As the *PRA1* gene family in plants has been poorly documented, putative PRA1 homologs were investigated using BLAST and HMMER. PRA1 domain-containing proteins were identified from the set of annotated protein-coding genes from six species with complete genome sequences (Arabidopsis, poplar [*Populus trichocarpa*], rice [*Oryza sativa*], moss [*Physcomitrella patens*], and two green algae, *Ostreococcus tauri* and *Chlamydomonas reinhardtii*). In addition, nonplant homologs from a set of eukaryotic model species were added to study the evolution of this gene family in other kingdoms. Finally, the PRA1 homologs were classified with multiple sequence alignments and phylogenetic tree construction methods (see "Materials and Methods").

In Arabidopsis, a total of 19 *PRA1* (designated *AtPRA1*) genes were identified and grouped into eight clades (A–H). This classification was based on support values from different phylogenetic tree construction methods (Fig. 1). An overview of the proposed nomenclature and number of homologs per species and clade is presented in Table I. Structural protein analysis showed that all AtPRA1 proteins consist of 180 to 240 amino acid residues, with a predicted molecular mass ranging between 20 and 26 kD, and contain two or more transmembrane domains. The small size of the AtPRA1 proteins is a feature conserved in the human PRA1 (185 amino acids and 20.6 kD) and its yeast counterpart (176 amino acids and 19.4 kD). The number of *PRA1*-homologous genes was higher in Arabidopsis, poplar (19 members), and rice (11 members) than in more primitive plants, such as moss, *O. tauri*, and *C. reinhardtii* (eight, three, and two, respectively; Supplemental Table S1), but no plant-specific domains could be distinguished. Clades A and B grouped homologs from both land plants and green algae, the former being evolutionarily related to the animal *PRAF2* and *PRAF3* genes, whereas clades C to H contained homologs occurring only in flowering plants.

AtPRA1 Proteins Can Dimerize in Accordance with Their Phylogenetic Distribution

Animal PRA1 proteins have been shown to function either as monomers or through the formation of a multimeric complex (Liang et al., 2004; Schweneker et al., 2005). To test whether all AtPRA1 proteins might interact to form dimers, yeast two-hybrid-based interaction analyses were carried out. Interactions were assayed by the mating methodology (see "Materials and Methods"). The interaction between two proteins was considered positive when both reporter genes were activated (*His* and *LacZ*). In summary, most of the AtPRA1 proteins were able to form homodimers and heterodimers (Fig. 2, A–C). Based on the yeast two-hybrid data, two main interaction networks were identified (Fig. 2D). Family members belonging to the same clade presented a mostly similar interaction profile. All members from clade B interacted with one another and also with the only member of clade E. A smaller interaction network was also found among clades D, F, and G, but, in this case, some family members did not interact with any AtPRA1, while those present in the interaction network had distinct interaction profiles. No interaction was found for seven AtPRA1 proteins (Fig. 2D), among them AtPRA1.A1, AtPRA1.A2, and AtPRA1.A3, which are more closely related to the PRAF2 and PRAF3 animal counterparts (Fig. 1), possibly indicating that they act as monomers.

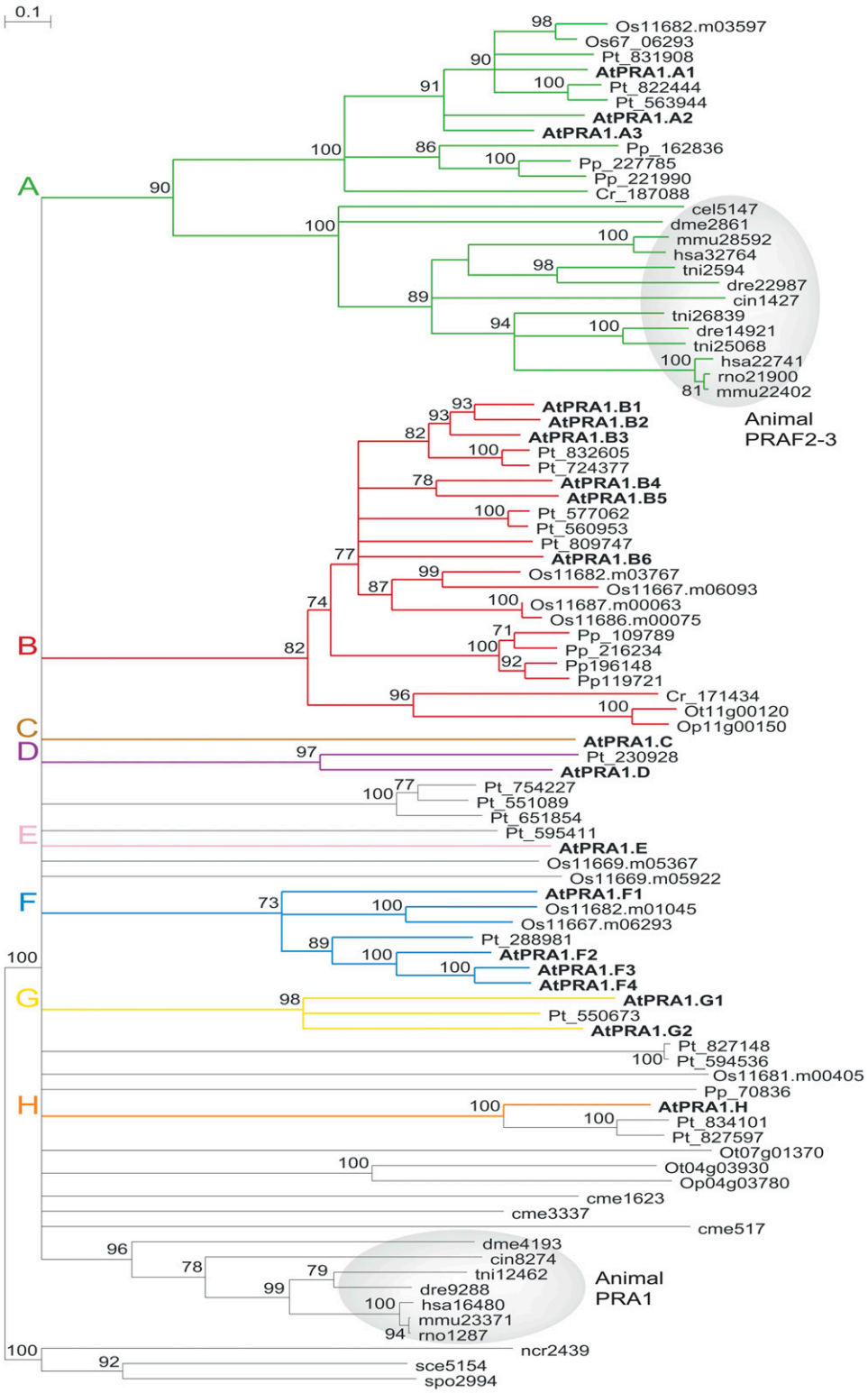

Figure 1. Neighbor-joining phylogenetic tree of eukaryotic PRA1 proteins. Proteins from Arabidopsis are in boldface, and proteins from other species are indicated by a two-letter prefix (Cr, *Chlamydomonas reinhardtii*; Op, *Ostreococcus lucimarinus*; Os, *Oryza sativa*; Ot, *Ostreococcus tauri*; Pp, *Physcomitrella patens*; Pt, *Populus trichocarpa*). Nonplant proteins are given with their original name from the OrthoMCL database (cel, *Caenorhabditis elegans*; cin, *Ciona intestinalis*; cme, *Cyanodioschyzon merolae* 10D; dme, *Drosophila melanogaster*; dre, *Danio rerio*; hsa, *Homo sapiens*; mmu, *Mus musculus*; ncr, *Neurospora crassa* OR74A; sce, *Saccharomyces cerevisiae* S288C; spo, *Schizosaccharomyces pombe*; tni, *Tetraodon nigroviridis*). Branches with fewer than 70% bootstrap were collapsed. The animal PRA1, PRAF2, and PRAF3 clusters are shaded in gray.

Table I. *Classification of AtPRA1 proteins*

Locus	Nomenclature	Predicted Transmembrane Domains[a]	Plant Taxonomic Distribution[b]	Subcellular Localization Pattern
Clade A			At:3, Pt:3, Os:2, Pp:3, Cr:1	
At5g02040	AtPRA1.A1	2 to 4		ER
At5g05987	AtPRA1.A2	2 to 4		Endosomal compartments
At3g11397	AtPRA1.A3	2 to 4		Endosomal compartments
Clade B			At:6, Pt5, Os:4, Pp:4, Ot:1, Cr:1	
At3g56110	AtPRA1.B1	2 to 5		Endosomal compartments
At2g40380	AtPRA1.B2	2 to 4		Endosomal compartments
At5g05380	AtPRA1.B3	2 to 5		Endosomal compartments
At2g38360	AtPRA1.B4	2 to 4		Endosomal compartments
At5g01640	AtPRA1.B5	2 to 4		Endosomal compartments
At5g07110	AtPRA1.B6	2 to 3		ER
Clade C			At:1	
At4g29658	AtPRA1.C	2 to 4		ER
Clade D			At:1, Pt:1	
At1g04260	AtPRA1.D	2 to 3		Endosomal compartments
Clade E			N.D., low bootstrap support	
At1g08770	AtPRA1.E	2 to 5		Endosomal compartments
Clade F			At:4, Pt:1, Os:2	
At1g17700	AtPRA1.F1	2 to 4		Endosomal compartments
At1g55190	AtPRA1.F2	2 to 4		Endosomal compartments
At3g13720	AtPRA1.F3	2 to 4		ER?[c]
At3g13710	AtPRA1.F4	2 to 4		Endosomal compartments
Clade G			At:2, Pt:1	
At1g55640	AtPRA1.G1	3 to 4		Endosomal compartments
At5g56230	AtPRA1.G2	2 to 4		ER?[c]
Clade H			At:1, Pt:2	
At4g27540	AtPRA1.H	2 to 3		ER

[a]Observed variation on transmembrane domain prediction was due to five different programs (see "Materials and Methods"). [b]N.D., Not determined. Two-letter species abbreviations are as described for Figure 1. [c]The AtPRA1.F3 and AtPRA1.G2 proteins showed indication of ER localization, but no strongly detectable GFP cells could be imaged.

Expression Analysis of *AtPRA1* Genes in Arabidopsis

To study the spatial control of *AtPRA1* gene expression, transgenic Arabidopsis plants were generated harboring the promoter region of *AtPRA1* genes fused to the *GUS* reporter gene. From the 19 *AtPRA1* genes, we were able to isolate the promoter region of 12 genes. As promoter sequence, we considered the intergenic region upstream of the start codon of the *AtPRA1* gene until the start or stop codon of the most upstream gene, with a maximum length of approximately 2 kb. From the progeny of transgenic T2 plants, only patterns observed in two independent lines were taken into account. For our analysis, we selected 8-d-old seedlings, because at this stage new organ structures arise and rapid growth is noticeable. This characteristic demands high vesicle activity, possibly linked to PRA1 regulation.

The obtained expression patterns are summarized in Table II. Expression was frequently observed in vascular tissues (Fig. 3, A–C). Four *AtPRA1* genes (*AtPRA1.B5*, *AtPRA1.B6*, *AtPRA1.D*, and *AtPRA1.E*) were expressed in leaf veins, with expression of *AtPRA1.B6* being restricted to young leaf veins (Fig. 3H). *AtPRA1.F3* had no GUS activity in any vascular tissues but shared a common distribution with other *AtPRA1* genes in regions of lateral root initiation (Fig. 3E). In roots, GUS staining was frequently observed at the lateral and/or the columella cells of the root cap (Fig. 3, M–O). Four *AtPRA1* genes (*AtPRA1.B5*, *AtPRA1.B6*, *AtPRA1.D*, and *AtPRA1.F3*) were expressed in both regions, while expression of *AtPRA1.B4* and *AtPRA1.E* was restricted to the lateral and the columella root cap cells, respectively. In aerial tissues, expression of *AtPRA1* genes was detected in trichomes (Fig. 3, J–L), stomata (Fig. 3, G–I), shoot apex (Fig. 3, F and J), and at the leaf base (Fig. 3D).

Comparison of expression profiles of members within the same clade revealed a high variability. For example, in clade B, five of its six members were analyzed for GUS activity. *AtPRA1.B1* was not expressed at the seedling stage (data not shown), but

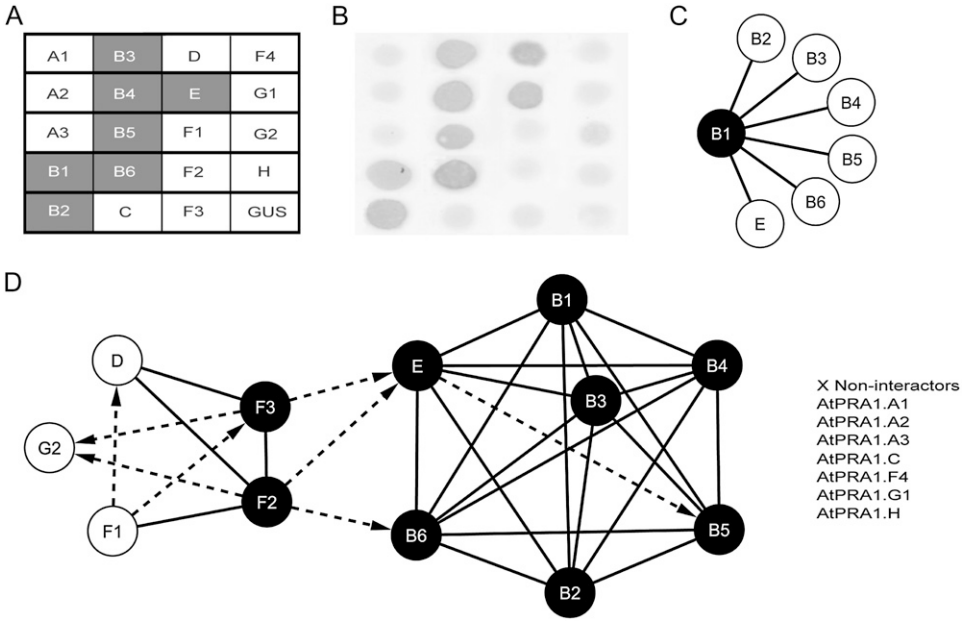

Figure 2. Yeast two-hybrid interactome of *AtPRA1* genes. A to C, Representative mating and β-galactosidase (X-Gal) assay results for AtPRA1.B1 to illustrate the methodology. A matrix was built on microtiter plates containing all prey, which were inoculated by independent bait constructs. The reporter gene encoding GUS was used as a negative control in all experiments. A, Mating assay for AtPRA1.B1. Positive interactions resulting from the activation of the reporter *His* gene are in gray. B, X-Gal assay for AtPRA1.B1. Positive X-Gal activities are in gray. C, Interaction network summarizing the final result for AtPRA1.B1. Nodes and connecting lines represent AtPRA1 proteins and interactions, respectively. The AtPRA1.B1 node is assigned in black to indicate homodimerization. The interaction was considered as positive only when both *His* and *LacZ* reporter genes were activated. D, Interaction network with all *AtPRA1* genes. Solid and dashed lines represent interactions in both directions and only one direction, respectively. Noninteractors are listed next to the network.

AtPRA1.B3 to *AtPRA1.B6* had an overlapping expression profile in the vascular tissues as well as expression patterns unique to the different family members. Although *AtPRA1.B4* and *AtPRA1.B6* were coexpressed in stomata, only *AtPRA1.B4* was detected in developed trichomes. Curiously, members from other clades (*AtPRA1.F2* and *AtPRA1.G2*) also showed GUS activity in trichomes, although for *AtPRA1.G2* it was restricted to the initiation stage, in clear contrast to the *AtPRA1.B4* expression.

AtPRA1 Genes Are Coexpressed with Rabs

With the accumulation of Arabidopsis gene expression data, regulatory and functional relationships between coexpressing genes can be explored (for review, see Aoki et al., 2007). Here, gene functions for the *AtPRA1* genes were inferred by comparison of gene expression profiles and GO enrichment analysis (see "Materials and Methods"). Using *AtPRA1* genes as guides for a genome-wide search, we found that genes

Table II. *Summary of histochemical GUS activity of 12 AtPRA1 promoter fusions in Arabidopsis seedlings*

Seedling	Vascular Tissues			Ground Tissues			Aerial Tissues			
	Hypocotyl	Root	Leaf	Lateral Root	Lateral Root Cap	Columella Cell	Trichome	Stomata	Shoot Apex	Leaf Base
AtPRA1.B1:GUS	−	−	−	−	−	−	−	−	−	−
AtPRA1.B3:GUS	+	−	−	−	−	−	−	−	+	−
AtPRA1.B4:GUS	−	+	−	+	+	−	+	+	−	−
AtPRA1.B5:GUS	−	+	+	+	+	+	−	−	+	−
AtPRA1.B6:GUS	+	+	+	+	+	+	−	+	−	−
AtPRA1.D:GUS	+	+	+	+	+	+	−	−	+	−
AtPRA1.E:GUS	+	+	+	+	−	+	−	−	+	−
AtPRA1.F1:GUS	+	−	−	−	−	−	−	−	+	+
AtPRA1.F2:GUS	+	−	−	−	−	−	+	−	−	−
AtPRA1.F3:GUS	−	−	−	+	+	+	−	−	−	−
AtPRA1.G1:GUS	−	+	−	+	−	−	−	−	−	−
AtPRA1.G2:GUS	−	+	−	−	−	−	+	−	−	−

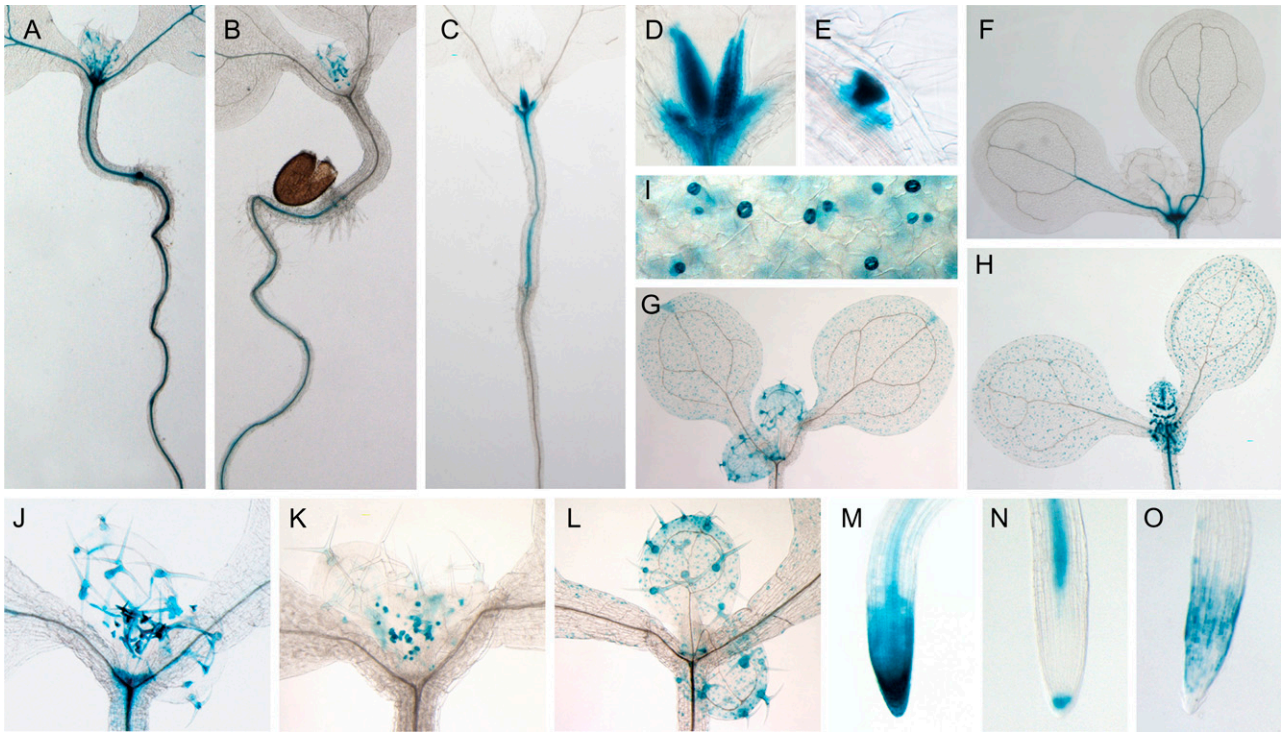

Figure 3. Activity of AtPRA1 promoter-GUS fusions (AtPRA1:GUS) in 8-d-old transgenic Arabidopsis seedlings. Representatives from each observed pattern are summarized. A, *AtPRA1.D*:*GUS* expression throughout the leaf veins, hypocotyl, and root tissues. B, *AtPRA1.G2*:*GUS* expression in vascular root tissues. C, *AtPRA1.F1*:*GUS* expression restricted to the hypocotyl region. D, Close-up of *AtPRA1.F1*:*GUS*, showing *GUS* expression at the leaf base. E, Expression of *AtPRA1.F3*:*GUS* at the lateral root primordium. F, *AtPRA1.E*:*GUS* expression in leaf veins and apical meristem. G and H, Expression of *AtPRA1.B4*:*GUS* and *AtPRA1.B6*:*GUS* in guard cells. Note the staining of trichomes of *AtPRA1.B4*:*GUS* and *AtPRA1.B6*:*GUS* at the leaf veins restricted to the developing leaf pair. I, Close-up of stomatal expression of *AtPRA1.B4*:*GUS*. J, *AtPRA1.F2*:*GUS* expression throughout trichomes and at the apical meristem as well. K, Staining of *AtPRA1.G2*:*GUS* restricted to initiating trichomes. L, *AtPRA1.B4*:*GUS* expression in fully developed trichomes. M, *AtPRA1.D*:*GUS* expression in columella and root cap cells. N, *AtPRA1.E*:*GUS* observed at the vascular root tissue and at the columella root cap cells. O, Localization of *AtPRA1.B4*:*GUS* expression in the root cap.

coexpressing with *AtPRA1* genes were significantly enriched for genes involved in "Golgi vesicle transport" and the "secretory pathway" (>6-fold enrichment, $P < 1e\text{-}10$). When focusing on the putative biological interaction between the AtPRA1 proteins and Rabs, we found that 10 of the 12 *AtPRA1* genes represented on the Affymetrix ATH1 microarray coexpressed with at least one Rab GTPase gene (Table III). Six of the 12 *AtPRA1* genes were coexpressed with more than one Rab GTPase, a feature that is not expected by chance ($P < 0.01$; Table III).

Subcellular Localization of the AtPRA1 Proteins in Arabidopsis

Our in silico search for the biological function of the AtPRA1s strongly suggested that these proteins, like Rabs, are involved in vesicle trafficking. In human, yeast, and mouse, PRA1 resides predominantly in the Golgi apparatus (Liang and Li, 2000; Huh et al., 2003; Sivars et al., 2003). However, PRA1 proteins have been reported in different trafficking compartments, such as the ER (Abdul-Ghani et al., 2001; Schweneker et al., 2005; Liu et al., 2006), synaptic vesicles (Fenster et al., 2000), COPI and COPII vesicles (Otte et al., 2001; Gilchrist et al., 2006), and endosomes (Schweneker et al., 2005; Geerts et al., 2007). To determine the subcellular localization of the 19 AtPRA1 proteins, their full-length open reading frames were fused to the enhanced GFP reporter protein (EGFP) and stably produced in Arabidopsis seedlings. As a control, the observed patterns were compared with those of seedlings harboring a vector expressing free EGFP. All AtPRA1 localization patterns were confirmed in tobacco (*Nicotiana benthamiana*) leaf epidermal cells that transiently expressed the respective *AtPRA1*:*GFP* fusions (Supplemental Figs. S1–S3).

As a general distribution pattern (Table I), we observed that most of the AtPRA1 proteins (AtPRA1.A2, AtPRA1.A3, AtPRA1.B1, AtPRA1.B2, AtPRA1.B3, AtPRA1.B4, AtPRA1.B5, AtPRA1.D, AtPRA1.E, AtPRA1.F1, AtPRA1.F2, AtPRA1.F4, and AtPRA1.G1)

Table III. *Coexpression analysis of AtPRA1 and Rab GTPase genes*

The *P* value indicates that the *AtPRA1* guide gene coexpresses with more Rabs than expected by chance (given the frequency of 0.3% or 57 Rabs in the Arabidopsis genome). Enrichment folds were calculated as the ratio of the relative occurrence in the set of coexpressed genes to that in the genome.

AtPRA1 Gene Guide	Rabs/Coexpressed Genes	*P*	Enrichment Fold
AtPRA1.A1	11/461	2.85E-08	8.98
AtPRA1.B1	9/425	1.61E-06	7.97
AtPRA1.B4	1/70	Not significant	5.37
AtPRA1.B6	10/427	1.57E-07	8.81
AtPRA1.D	0/10	Not significant	0.00
AtPRA1.E	0/10	Not significant	0.00
AtPRA1.F1	1/33	Not significant	11.40
AtPRA1.F2	1/38	Not significant	9.90
AtPRA1.F3	5/214	2.57E-04	8.79
AtPRA1.G1	3/74	1.01E-03	15.25
AtPRA1.G2	3/373	Not significant	3.03
AtPRA1.H	6/256	5.85E-05	8.82

localized to vesicular structures often associated with a light network of ER strands (Fig. 4; Supplemental Fig. S1, B–H and K–P). Representatives from different clades were selected to investigate these structures. The localization of AtPRA1.A2, AtPRA1.B5, AtPRA1.D, AtPRA1.E, AtPRA1.F1, and AtPRA1.G1 in endosomal compartments was confirmed in Arabidopsis seedlings by colocalization experiments with the endocytic tracer *N*-(3-triethylammoniumpropyl)-4-(6-(4-(diethylamino)-phenyl)hexatrienyl)pyridinium dibromide (FM4-64; Brandizzi et al., 2004; Fig. 4). For a small subset (AtPRA1.A1, AtPRA1.B6, AtPRA1.C, and AtPRA1.H), the fluorescence marked a well-structured strand network, clearly indicative of the ER (Fig. 5B; Supplemental Fig. S1, A, I, J, and Q). The ER localization of the AtPRA1 proteins was similar to the distribution of a chimeric ER marker that contained a HDEL signal at the C terminus of the fluorescent reporter protein and the signal peptide AtWAK2 at the N terminus (Nelson et al., 2007) and was clearly distinct from the free EGFP protein accumulation pattern (Fig. 5A). As shown for AtPRA1.B6, the ER distribution was further confirmed by colocalization experiments in tobacco (Supplemental Fig. S3). Also, AtPRA1.F3 and AtPRA1.G2 localizations suggested GFP fluorescence in the ER, but no clear conclusion could be drawn due to the low expression levels of the reporter gene constructs (data not shown).

Because most of the PRA1 family members localized to endosomal vesicles, we investigated the identity of these compartments. Representative AtPRA1 proteins from clades B, D, E, and F were selected for colocalization analysis in tobacco. We used fluorescence-tagged organelle markers for cis-Golgi (Man49:mCherry; Nelson et al., 2007) and endosomal/prevacuolar compartments (PVCs; mRFP:AtRabF2b). Recently, the AtRabF2b protein was shown to identify sorting endosomes that redirect trafficking between secretory and endocytic pathways (Jallais et al., 2008). All of the analyzed AtPRA1 proteins colabeled with the used markers, albeit to a different extent (Figs. 6 and 7). None of the analyzed AtPRA1 proteins resided entirely in the Golgi compartment (Fig. 6). However, the B-clade members were more distributed over the Golgi apparatus than those of other clades (Fig. 6A). Since the Man49:GFP construct also labeled the ER when expressed in tobacco leaf epidermal cells, as demonstrated previously (Saint-Jore-Dupas et al., 2006), we repeated the colocalization experiments with the rat sialyltransferase (ST:RFP) Golgi marker (Munro, 1991), with corroborative results for the Golgi localization (data not shown). Interestingly, members of clades D and F entirely overlapped the endosomal/PVC marker AtRabF2b (Fig. 7, B and D). The single member of clade E colocalized with both markers, without clear preference for the Golgi or endosomes (Figs. 6C and 7C).

DISCUSSION

Proteins containing a PRA1 domain have been found in different organisms, mainly interacting with proteins involved in vesicle trafficking or with viral proteins (Compton and Behrend, 2006). Here, we initiated a functional characterization of the *PRA1* gene family in Arabidopsis. Although we were unable to detect a direct or indirect interaction between AtPRA1 proteins and Rabs through yeast two-hybrid and tandem affinity purification (data not shown), our in silico coexpression analysis and subcellular localization data indicate an important role for AtPRA1 proteins in the trafficking pathways in plants. Plants possess a significantly larger number of PRA1 domain-containing proteins than animals. The presence of multiple isoforms is not an unprecedented attribute for constituents of the vesicle transport machinery in plants, as seen for the small GTPases and the superfamily of SNARE proteins (Bassham and Raikhel, 2000; Vernoud et al., 2003; Sutter et al., 2006). Comparative genome

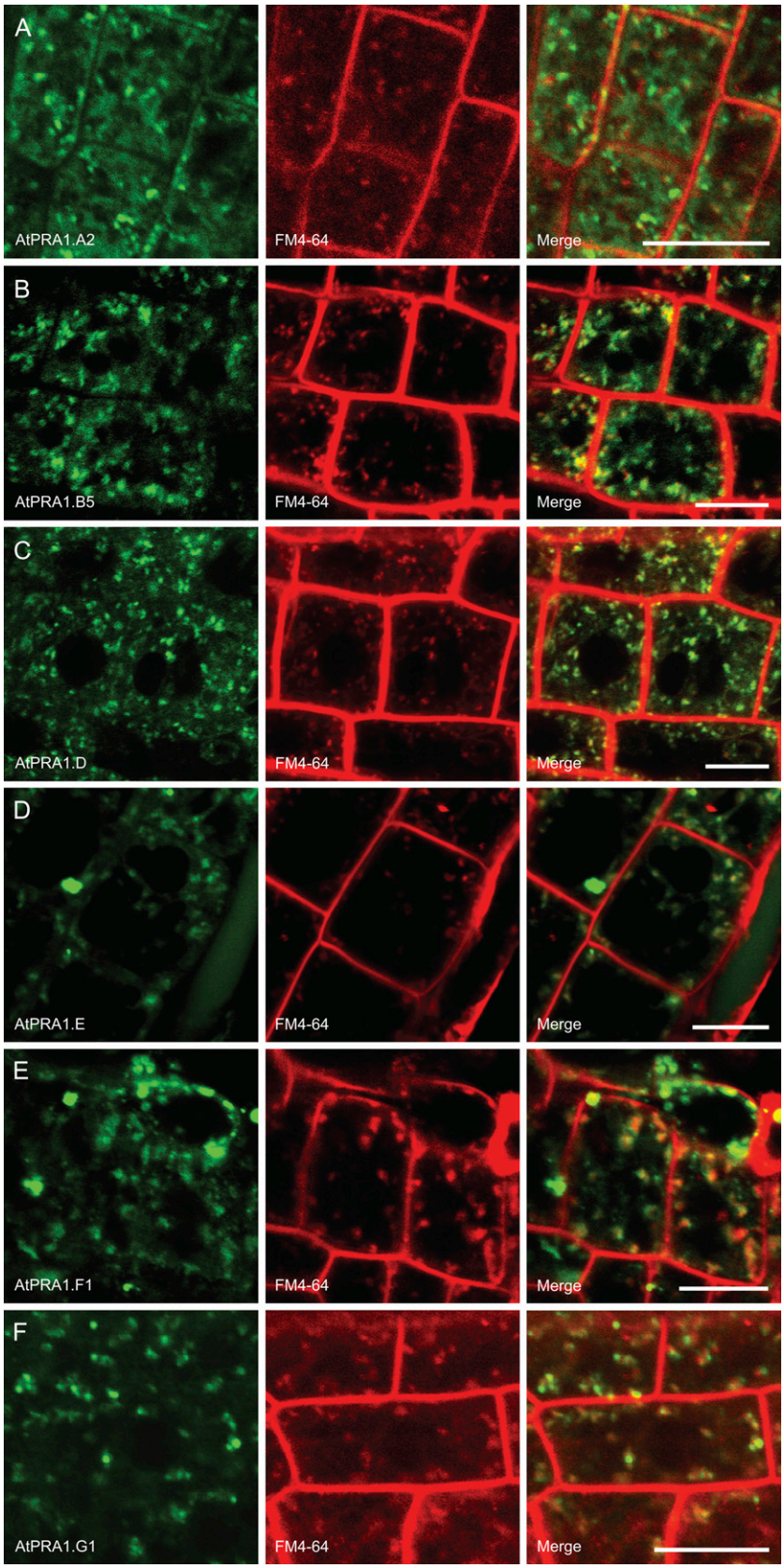

Figure 4. Subcellular distribution pattern of AtPRA1 proteins over endosomes in stable transgenic Arabidopsis root cells. Representatives from each clade are presented; for the localization pattern of all AtPRA1 proteins in tobacco, see Supplemental Figure S1. Seedlings were treated for 15 to 30 min with the fluorescent dye FM4-64, which is a reliable tracer for the endocytic trafficking in Arabidopsis root cells (Russinova et al., 2004; Dettmer et al., 2006; Reichardt et al., 2007). A, AtPRA1.A2. B, AtPRA1.B5. C, AtPRA1.D. D, AtPRA1.E. E, AtPRA1.F1. F, AtPRA1.G1. Bars = 10 μm.

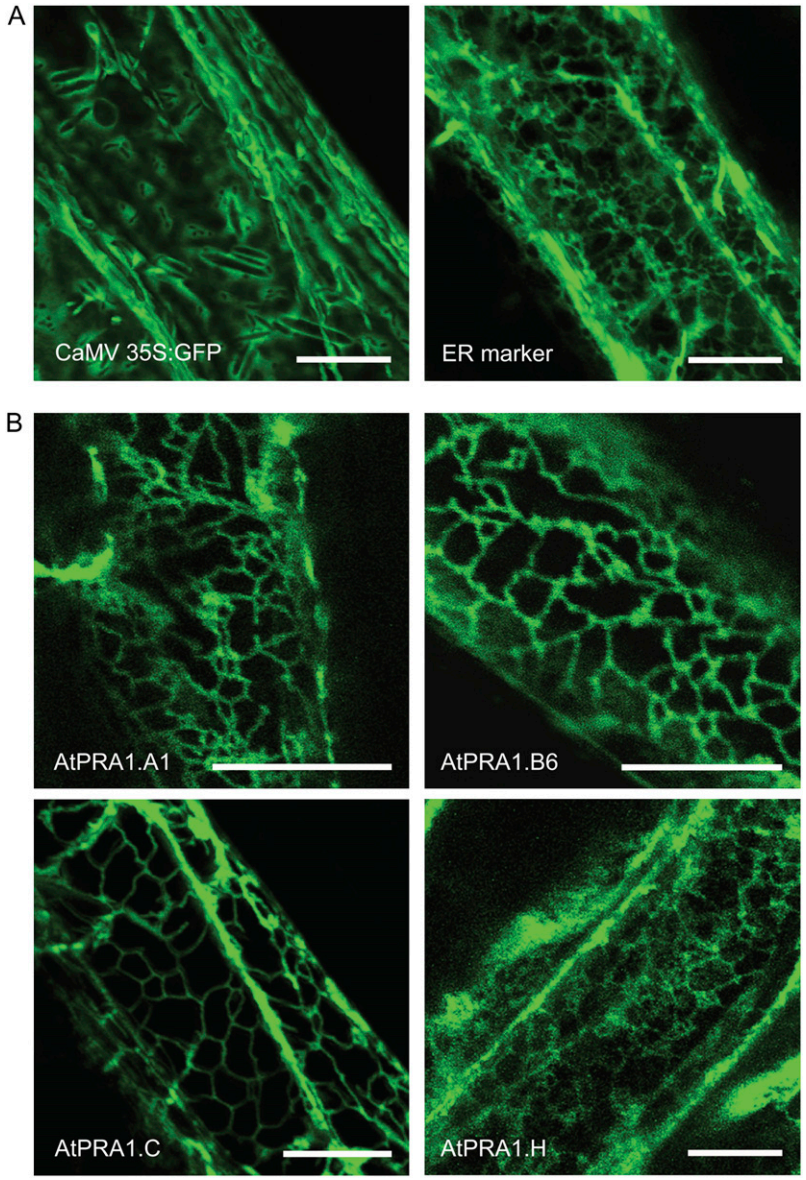

Figure 5. Subcellular distribution pattern of AtPRA1 proteins over ER in stable transgenic Arabidopsis root cells. A, Negative and positive control seedlings harboring the vector CaMV 35S:GFP and the ER marker tagged to GFP, respectively. The adopted ER marker corresponds to a chimeric fusion of the signal peptide AtWAK2 and the HDEL retention signal to the fluorescent marker gene. B, The four AtPRA1 proteins showing ER localization. Bars = 10 μm.

analysis has previously suggested that plants have evolved unique features in vesicle trafficking, probably to attend plant-specific requirements (Assaad, 2001; Rutherford and Moore, 2002). This feature might be related to the rather complex vacuolar system of plants, in contrast to that of other eukaryotes. Thus, the presence of a more sophisticated vesicle-trafficking machinery in plants is not surprising, but whether the expansion of the Arabidopsis *PRA1* family reflects functional diversification or redundancy still needs to be examined. The spatial expression analysis and subcellular localization data suggest both possibilities. Whereas the distinct expression patterns hint at tissue-specific specification of certain AtPRA1 members (an almost nonoverlapping tissue-specific expression pattern is observed for three members of the F clade), the diverse subcellular localization patterns indicate that different PRA1 proteins might work in specific steps of vesicle trafficking. By partitioning the tasks, PRA1 isoforms could attend more efficiently and specifically to the demand of a complex trafficking system. Moreover, based on the yeast two-hybrid results, it is not unlikely that AtPRA1 proteins might aggregate as heterodimers to gain specificity.

The literature validates the view of PRA1s as elaborate proteins, capable of operating as monomers, dimers, or trimers. Mouse PRA1 export from the ER to the Golgi was shown to depend on homodimerization (Liang et al., 2004). The PRA1 domain-containing protein Jena-Muenchen 4 (JM4) forms a multimeric complex (Schweneker et al., 2005). We have observed homodimerization and heterodimerization among members of the AtPRA1 family. The obtained interaction network is in accordance with the phylogenetic

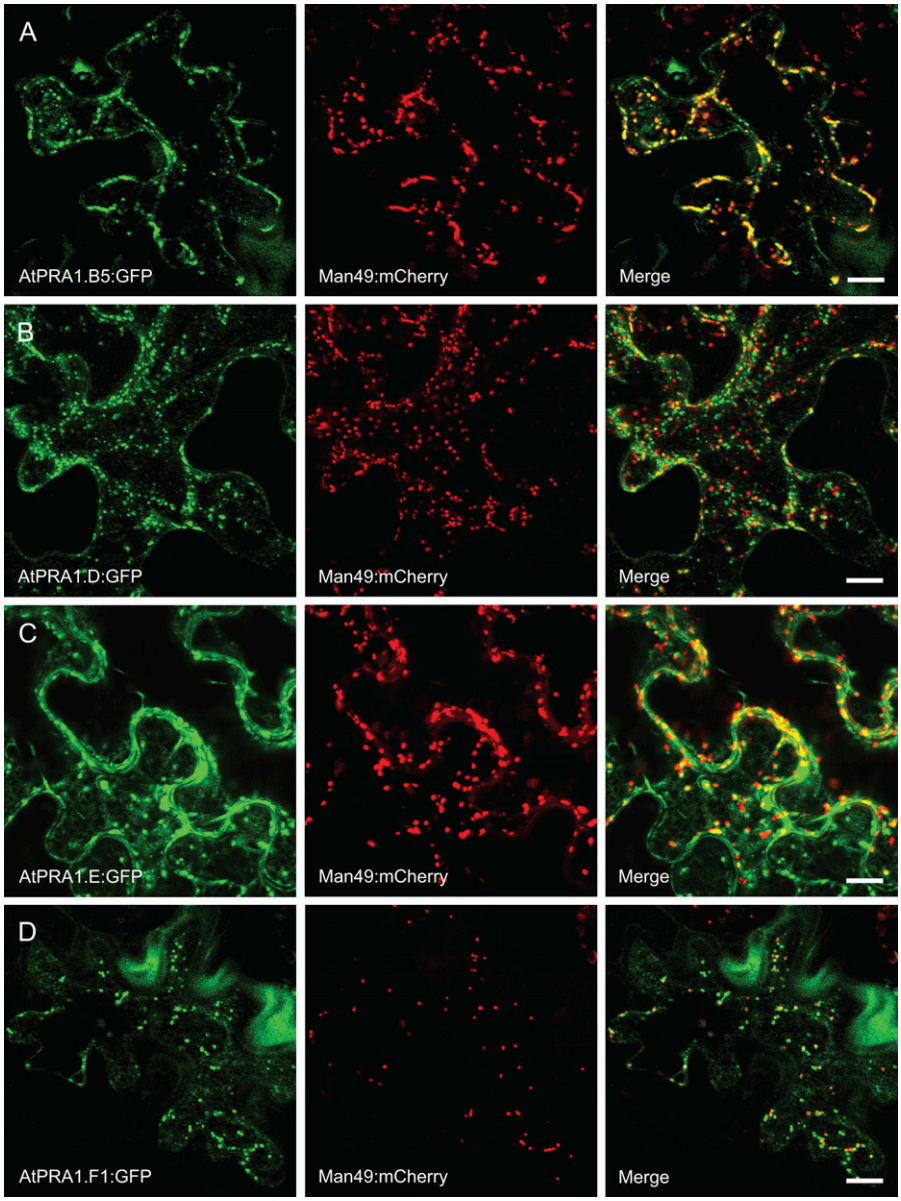

Figure 6. Colocalizations of AtPRA1.B5, AtPRA1.D, AtPRA1.E, and AtPRA1.F1 with the Man49:mCherry cis-Golgi marker. All AtPRA1 proteins showed double labeling with the used markers, in a degree dependent on the observed clades. The B-clade members were more distributed over the Golgi apparatus than members of the other clades. Bars = 10 μm.

distribution of the AtPRA1 proteins, showing mainly interactions between the less diverged members. Different *AtPRA1* genes were expressed frequently in the same tissues and cellular compartments, corroborating the view of family members cooperating in specific processes. For some AtPRA1 proteins, no dimerization was found, which might indicate that they are functionally divergent from the other AtPRA1 proteins.

PRA1 proteins are frequently reported as Golgi proteins in human, yeast, and mouse (Liang and Li, 2000; Huh et al., 2003; Sivars et al., 2003). Our subcellular localization data revealed that AtPRA1 is distributed over endosomal compartments, preferentially over the cis-Golgi and the endosomal/PVC compartments. Interestingly, with the exception of members of the D and F clades that overlapped with the endosomal/PVC marker mRFP:AtRabF2b, the AtPRA1 proteins and the adopted subcellular localization markers only partially colocalized, with the degree of overlay depending on the AtPRA1 studied. This is not the first time that a PRA1 protein was found simultaneously in different compartments within the same cell. The human PRA1 domain-containing protein JM4 is present in the trans-Golgi, endosomes, and ER (Schweneker et al., 2005). In yeast, Yip3p was found in COPII vesicles through mass spectrometry (Otte et al., 2001), while rat PRA1 was identified in Golgi and COPI vesicles (Gilchrist et al., 2006). The use of extra markers, such as the trans-Golgi network marker vacuolar H^+-ATPase subunit a1 (Dettmer et al., 2006), will help address more precisely the role of AtPRA1 proteins in vesicle-trafficking compartments.

Some AtPRA1 family members (AtPRA1.A1, AtPRA1.B6, AtPRA1.C, and AtPRA1.H) were found

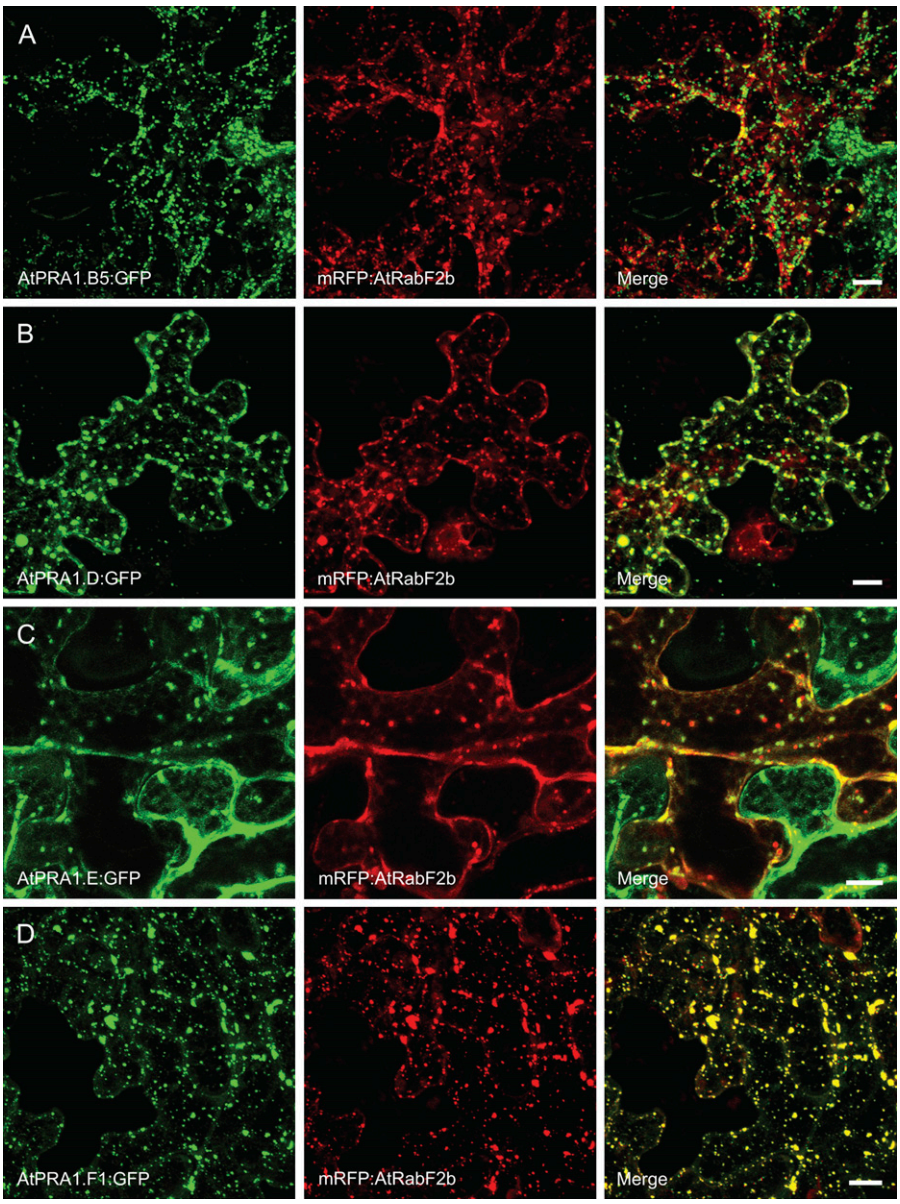

Figure 7. Colocalizations of AtPRA1.B5, AtPRA1.D, AtPRA1.E, and AtPRA1.F1 with the mRFP:AtRabF2b endosomal/PVC marker. All AtPRA1 proteins showed double labeling with the used markers, in a degree dependent on the observed clades. Note that D- and F-clade members entirely colabeled with the endosomal/PVC marker AtRabF2b. Bars = 10 μm.

to reside in the ER. To our knowledge, this is the first time that PRA1 isoforms have been observed uniquely in the ER compartment. When labeled ER strands are observed together with vesicles, the ER localization cannot be excluded as a consequence of the use of the strong CaMV 35S promoter. However, the weak ER labeling might also result from the recycling of Golgi proteins through the ER (Brandizzi et al., 2002). Indeed, in human cells infected with the Epstein-Barr virus, PRA1 regulates the trafficking of the latent membrane protein 1 from the ER to the Golgi (Liu et al., 2006). In this scenario, the association between the specific ER-resident AtPRA1.B6 and other B-clade AtPRA1 proteins might be explained. To confirm this hypothesis, the AtPRA1 distribution on other compartments, such as the COP vesicles, remains to be explored.

Regarding the spatial distribution, PRA1 homologs have been ubiquitously found in human tissues, emphasizing their importance for development (Martincic et al., 1997; Abdul-Ghani et al., 2001; Bucci et al., 2001; Schweneker et al., 2005; Fo et al., 2006). Based on our results in 8-d-old seedlings, *AtPRA1* transcripts are differently distributed, mainly accumulating in emerging organs and vascular tissues. Intense vesicle trafficking is expected to take place at sites where rapid membrane and cell wall synthesis is needed. In agreement, for two B-clade members, expression was observed in stomata, trichomes, and vascular tissues. Guard cells are exposed to frequent volume changes due to water uptake, associated with membrane internalization and remobilization (Shope and Mott, 2006). Expression of *AtPRA1* genes during

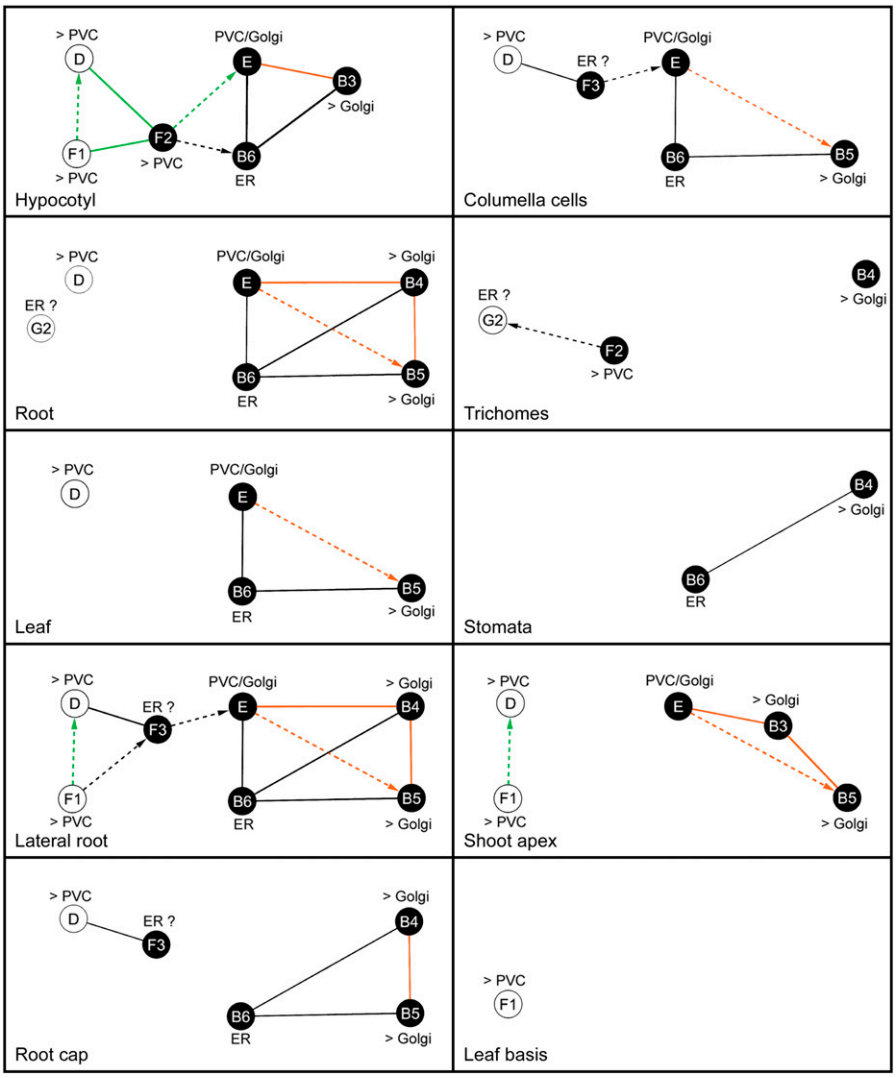

Figure 8. Tissue- and subcellular-based AtPRA1 protein interaction maps. In accordance to the spatial distribution of the 12 *AtPRA1* genes observed in 8-d-old Arabidopsis seedlings, the interactome and the subcellular localization data are depicted for every tissue in which the *AtPRA1* genes were expressed. Nodes colored black indicate homodimerization. Solid and dashed lines represent interactions in both directions and only one direction, respectively. Interacting proteins localized in the same subcellular compartment are highlighted in orange or green, corresponding to the Golgi and PVC, respectively. Question marks indicate the two AtPRA1 proteins (AtPRA1.F3 and AtPRA1.G2) that showed expression indicative of ER localization, but no strong detectable GFP cells were found to be imaged (data not shown). AtPRA1.D, AtPRA1.F1, and AtPRA1.F3 showed preferential localization over the endosomes/PVC (>PVC). AtPRA1.B1, AtPRA1.B2, AtPRA1.B3, AtPRA1.B4, and AtPRA1.B5 showed preferential localization over the cis-Golgi compartment (>Golgi). AtPRA1.B6 displayed distribution restricted to the ER, while AtPRA1.E showed no preference for the Golgi or endosome compartments (PVC/Golgi).

trichome development is probably related to changes in cell morphology during growth. This process depends intimately on cell wall expansion and deposition of new wall material by exocytosis. Regarding the vascular tissue expression, an ADP-ribosylation factor GTPase-activating protein has been shown to be required for normal vein patterning (Koizumi et al., 2005). The vascular localization of AtPRA1 proteins could be linked to cell wall thickening to overcome the turgor. Thus, the expression of *AtPRA1* genes in stomata, trichomes, and vascular tissues suggests that they might be involved mainly in the control of rapid cell expansion and growth.

In conclusion, the presented data reveal the participation of AtPRA1 proteins in the intracellular transport pathway. Members from the same clade have similar subcellular distribution, but their diverse spatial expression patterns suggest specification. Based on our observations, several models are proposed to describe the putative interactions between AtPRA1s for different subcellular compartments in different tissues of 8-d-old seedlings (Fig. 8). The complexity of these models seems to depend on the tissue examined, being highly connected in hypocotyls and lateral roots but simple in tissues in which few *AtPRA1* genes are expressed, as in stomata and at leaf bases. It is likely that in hypocotyls and lateral roots, AtPRA1 proteins function on both secretory and endocytic pathways, converging at the PVC compartments (Fig. 8). Interactions observed in the AtPRA1 interactome, but not covered by these models, might occur during other developmental processes in which Rabs are highly active, such as in root hairs or pollen tubes (Šamaj et al., 2006). Additional independent biochemical assays and more detailed fractionation studies might help test the proposed models.

MATERIALS AND METHODS

Sequence Analysis

Predicted proteins were downloaded from www.arabidopsis.org (Arabidopsis [*Arabidopsis thaliana*]), www.tigr.org (rice [*Oryza sativa*]), www.jgi.doe.gov (poplar [*Populus trichocarpa*], moss [*Physcomitrella patens*], *Ostreococcus*

lucimarinus, and *Chlamydomonas reinhardtii*), and bioinformatics.psb.ugent.be (*Ostreococcus tauri*). All other eukaryotic protein sequences were retrieved from the OrthoMCL Database (orthomcl.cbil.upenn.edu). The program hmmsearch from the HMMER package together with the PRA1 PFAM domain (PF03208) was used to identify putative *PRA1* genes, as were BLASTP searches with known *PRA1* genes. Protein sequences were aligned with T-Coffee (Notredame et al., 2000) and manually edited with BioEdit (Hall, 1999; for sequence alignment, see Supplemental Fig. S5). Neighbor-joining phylogenetic trees were constructed with TreeCon (Van de Peer and De Wachter, 1993) based on Poisson-corrected evolutionary distances with 1000 bootstrap samples. Maximum likelihood trees were created with TREE-PUZZLE (Schmidt et al., 2002) with 50,000 puzzling steps and with γ-distributed rates (eight categories) to model rate heterogeneity, which yielded a similar clade classification (data not shown).

Coexpression Analysis

Based on a compiled Arabidopsis ATH1 expression compendium containing 489 microarray experiments (Vandepoele et al., 2006), pairwise gene coexpression relationships were determined with the Pearson correlation coefficient (PCC). With a guide gene approach, all genes coexpressed with a PCC $\geq$ 0.279 were selected to evaluate the enrichment for GO categories. This PCC threshold was selected because it had the best gene function prediction power given the properties of this expression compendium (data not shown). GO associations for Arabidopsis proteins were retrieved from The Arabidopsis Information Resource. The gene assignments to the original GO categories were extended to include parental terms (i.e. a gene assigned to a given category was automatically assigned to all of the parent categories as well). All GO categories containing fewer than 20 genes were discarded from further analysis. Enrichment folds were calculated as the ratio of the relative occurrence in a set of genes to that in the genome. The statistical significance of the functional enrichment within sets of genes was evaluated with the hypergeometric distribution adjusted by the Bonferroni correction for multiple hypothesis testing. Corrected P values of <0.05 were considered significant.

Plant Growth Conditions and Plasmid Construction

Plants of Arabidopsis (ecotype Columbia) were grown under long-day conditions (16 h of light, 8 h of darkness) at 22°C on half-strength Murashige and Skoog germination medium (Murashige and Skoog, 1962). Wild-type tobacco (*Nicotiana benthamiana*) plants were grown under a normal light regime (14 h of light, 10 h of darkness) at 25°C and 70% relative humidity. The full-length open reading frames of all *AtPRA1* genes with and without stop codon were amplified from Arabidopsis genomic DNA or cDNA by PCR (for primer sequences, see Supplemental Table S2) and cloned into pDONR221 ENTRY vector by attB $\times$ attP (BP) recombination reaction according to the manufacturer's instructions (Invitrogen). The *AtPRA1* promoter sequences were amplified from Arabidopsis genomic DNA by PCR (for primer sequences, see Supplemental Table S2) or obtained from the systematic analysis of the Arabidopsis promoterome database (Benhamed et al., 2008). Each PCR fragment was cloned into the pDONRP4P1R entry vector by BP reaction and subsequently transferred into the pMK7S*NFm14GW modular destination vector (Karimi et al., 2007) by attL $\times$ attR (LR) recombination reaction, resulting in a transcriptional fusion between the *AtPRA1* promoters and the *EGFP-GUS* fusion. All constructs were transferred into the *Agrobacterium tumefaciens* C58C1Rif^R strain harboring the pMP90 plasmid. The obtained *Agrobacterium* strains were used to generate stably transformed Arabidopsis with the floral dip transformation method (Clough and Bent, 1998). Transgenic plants were cultured on kanamycin-containing medium and later transferred to soil.

Yeast Two-Hybrid Experiments

Yeast two-hybrid bait and prey vectors were obtained through recombinational Gateway cloning (Invitrogen). All *AtPRA1* full-length open reading frames were recombined into the pDEST22 and pDEST32 vectors (Invitrogen) by an LR reaction, resulting in translational fusions between the open reading frames and the GAL4 transcriptional activation and GAL4 DNA-binding domains, respectively. Plasmids encoding the baits and prey were transformed into the yeast strains PJ69-4α (MATα; trp1-901, leu2-3,112, ura3-52, his3-200, gal4Δ, gal80Δ, LYS2::GAL1-HIS3, GAL2-ADE2, met2::GAL7-lacZ) and PJ69-4a (MATa; trp1-901, leu2-3,112, ura3-52, his3-200, gal4Δ, gal80Δ, LYS2TGAL1-HIS3, GAL2-ADE2, met2TGAL7-lacZ) by the LiAc method (Gietz et al., 1992) and plated on synthetic dextrose (SD) plates without Leu and without Trp for 2 d at 30°C, respectively. Interactions between fusion proteins were assayed by the mating method. Diploid strains were transferred to SD medium without Leu and Trp (as a control) and to SD medium without Leu, Trp, and His. Plates were incubated at 30°C and scored for yeast growth by measuring the optical density (OD) of the cultures. By dividing the OD of the SD medium without Leu, Trp, and His by that without Leu and Trp but with His, a percentage of protein-protein interaction was obtained. A LacZ test was done to check for self-activators.

GUS Assay

Eight-day-old seedlings were stained on microtiter plates (Falcon 3043; Becton-Dickinson) and assayed for GUS as described (Beeckman and Engler, 1994). The reactions were carried out at 37°C in the dark for 4 h to overnight. Samples mounted in lactic acid were observed and photographed with a differential interference contrast microscope (Leica).

Fluorescent Marker Constructs, Confocal Microscopy, and Image Analysis

Full-length open reading frames of all *AtPRA1* genes were transferred into the pK7FWG2 (or pK7WGF2) destination vector (Karimi et al., 2002) by LR reaction, resulting in a set of transcriptional fusions between the CaMV *35S* promoter and *EGFP:AtPRA1.A1*, *EGFP:AtPRA1.A2*, *EGFP:AtPRA1.A3*, *AtPRA1.B1:EGFP*, *AtPRA1.B2:EGFP*, *AtPRA1.B3:EGFP*, *AtPRA1.B4:EGFP*, *AtPRA1.B5:EGFP*, *AtPRA1.B6:EGFP*, *EGFP:AtPRA1.C*, *AtPRA1.D:EGFP*, *EGFP:AtPRA1.E*, *AtPRA1.F1:EGFP*, *AtPRA1.F2:EGFP*, *AtPRA1.F3:EGFP*, *AtPRA1.F4:EGFP*, *AtPRA1.G1:EGFP*, *AtPRA1.G2:EGFP*, and *EGFP:AtPRA1.H* fusion genes. All constructs were transferred into the *Agrobacterium* C58C1Rif^R strain harboring the pMP90 plasmid. The obtained *Agrobacterium* strains were used for transient expression analysis in tobacco by leaf infiltration and to generate stably transformed Arabidopsis with the floral dip transformation method (Clough and Bent, 1998). The control vector expressing free GFP, the marker mRFP:AtRabF2b, and the Arabidopsis seeds harboring the construct CaMV 35S:GFP were already available in our collection. Other markers used in this study (ER and cis-Golgi) and the seeds expressing the ER:GFP marker were a kind gift of A. Nebenführ (University of Tennessee, Knoxville). The ER marker construct resulted from the combination of the fluorescent gene flanked by the signal peptide of AtWAK2 (He et al., 1999) and the ER retention signal HDEL at the N and C termini, respectively. The Golgi localization was based on the cytoplasmic tail and transmembrane (first 49 amino acids) of GmMan1, soybean (*Glycine max*) α-1,2-mannosidase I, as described previously (Saint-Jore-Dupas et al., 2006). For FM4-64 staining, the FM4-64 dye was dissolved in water at a final concentration of 4 mM. Seedlings were incubated at room temperature for 15 to 30 min. The transient expression assay on tobacco leaves was done according to Batoko et al. (2000) with minor modifications. In brief, the transformed *Agrobacterium* harboring the *AtPRA1* or marker constructs was grown for 2 d in a shaking incubator (200 rpm) at 28°C in 5 mL of yeast extract beef medium supplemented with appropriate antibiotics. Of the cultures, 2 mL was transferred to Eppendorf tubes and centrifuged (10 min, 5,000*g*), and the pellets were washed twice with 1 mL of infiltration buffer (50 mM MES, pH 5.6, 2 mM Na_3PO_4, and 0.5% Glc). The final pellet was resuspended in the infiltration buffer supplemented with 100 μM acetosyringone. The bacterial suspension was diluted with the same supplemented buffer to adjust the inoculum concentration to the final OD_{600} value. For coexpression experiments, 500 mL of each bacterial culture was mixed prior to the leaf infiltration, with the inoculum of each construct adjusted to the required final OD_{600}. The inoculum was delivered to tobacco leaves by gentle pressure infiltration through the stomata of the lower epidermis with a 1-mL syringe without a needle. The infected area of the leaf was delimited and labeled with an indelible pen. The plant was incubated under normal growing conditions. Transformed leaves were assayed for fluorescence at 2 to 4 d after infiltration with a confocal microscope (Olympus FluoView FV1000) equipped with a 63$\times$ water-corrected objective (numerical aperture of 1.2) to scan the cells. Dual GFP and red fluorescent protein (RFP) fluorescence were sequentially imaged in a multichannel setting with 488- and 543-nm light for GFP and RFP excitation, respectively. Emission fluorescence was captured in the frame-scanning mode alternating GFP fluorescence via a 500-/550-nm bandpass emission filter and RFP via a 560-nm cutoff filter. Images were recorded at 1$\times$ to 8$\times$ digital zoom.

Supplemental Data

The following materials are available in the online version of this article.

Supplemental Figure S1. Subcellular distribution of AtPRA1 proteins in tobacco leaf epidermal cells.

Supplemental Figure S2. Subcellular distribution of free GFP proteins in tobacco epidermal cells.

Supplemental Figure S3. Subcellular distribution of AtPRA1.B6 over the ER in tobacco leaf epidermal cells.

Supplemental Figure S4. Sequence alignment of PRA1 proteins.

Supplemental Table S1. PRA1 HMMER search results.

Supplemental Table S2. Primer sequences.

ACKNOWLEDGMENTS

We thank Andreas Nebenführ for providing seeds and markers used for the colocalization analysis, Barbara Berckmans, Naoki Takahashi, Tim Lammens, and Véronique Boudolf for technical support and encouragement, all past and current members of the cell cycle group for fruitful discussions and suggestions, and Martine De Cock for help preparing the manuscript.

Received April 29, 2008; accepted June 25, 2008; published June 26, 2008.

LITERATURE CITED

Abdul-Ghani M, Gougeon P-Y, Prosser DC, Da-Silva LF, Ngsee JK (2001) PRA isoforms are targeted to distinct membrane compartments. J Biol Chem **276:** 6225–6233

Akiduki S, Ochiishi T, Ikemoto MJ (2007) Neural localization of addicsin in mouse brain. Neurosci Lett **426:** 149–154

Aoki K, Ogata Y, Shibata D (2007) Approaches for extracting practical information from gene co-expression networks in plant biology. Plant Cell Physiol **48:** 381–390

Assaad FF (2001) Of weeds and men: what genomes teach us about plant cell biology. Curr Opin Plant Biol **4:** 478–487

Bassham DC, Raikhel NV (2000) Unique features of the plant vacuolar sorting machinery. Curr Opin Cell Biol **12:** 491–495

Batoko H, Zheng H-Q, Hawes C, Moore I (2000) A Rab1 GTPase is required for transport between the endoplasmic reticulum and Golgi apparatus and for normal Golgi movement in plants. Plant Cell **12:** 2201–2217

Beeckman T, Engler G (1994) An easy technique for the clearing of histochemically stained plant tissue. Plant Mol Biol Rep **12:** 37–42

Benhamed M, Martin-Magniette M-L, Taconnat L, Bitton F, Servet C, De Clercq R, De Meyer B, Buysschaert C, Rombauts S, Villarroel R, et al (2008) Genome-scale Arabidopsis promoter array identifies targets of the histone acetyltransferase GCN5. Plant J (in press)

Bourne HR, Sanders DA, McCormick F (1990) The GTPase superfamily: a conserved switch for diverse cell functions. Nature **348:** 125–132

Brandizzi F, Iron SL, Johansen J, Kotzer A, Neumann U (2004) GFP is the way to glow: bioimaging of the plant endomembrane system. J Microsc Oxf **214:** 138–158

Brandizzi F, Snapp EL, Roberts AG, Lippincott-Schwartz J, Hawes C (2002) Membrane protein transport between the endoplasmic reticulum and the Golgi in tobacco leaves is energy dependent but cytoskeleton independent: evidence from selective photobleaching. Plant Cell **14:** 1293–1309

Bucci C, De Gregorio L, Bruni CB (2001) Expression analysis and chromosomal assignment of PRA1 and RILP genes. Biochem Biophys Res Commun **286:** 815–819

Clough SJ, Bent AF (1998) Floral dip: a simplified method for *Agrobacterium*-mediated transformation of *Arabidopsis thaliana*. Plant J **16:** 735–743

Compton SL, Behrend EN (2006) PRAF1: a Golgi complex transmembrane protein that interacts with viruses. Biochem Cell Biol **84:** 940–948

Derby MC, Gleeson PA (2007) New insights into membrane trafficking and protein sorting. Int Rev Cytol **261:** 47–116

Dettmer J, Hong-Hermesdorf A, Stierhof YD, Schumacher K (2006) Vacuolar H^+-ATPase activity is required for endocytic and secretory trafficking in *Arabidopsis*. Plant Cell **18:** 715–730

Fenster SD, Chung WJ, Zhai R, Cases-Langhoff C, Voss B, Garner AM, Kaempf U, Kindler S, Gundelfinger ED, Garner CC (2000) Piccolo, a presynaptic zinc finger protein structurally related to Bassoon. Neuron **25:** 203–214

Figueroa C, Taylor J, Vojtek AB (2001) Prenylated Rab acceptor protein is a receptor for prenylated small GTPases. J Biol Chem **276:** 28219–28225

Fo CS, Coleman CS, Wallick CJ, Vine AL, Bachmann AS (2006) Genomic organization, expression profile, and characterization of the new protein PRA1 domain family, member 2 (PRAF2). Gene **371:** 154–165

Geerts D, Wallick CJ, Koomoa D-LT, Koster J, Versteeg R, Go RCV, Bachmann AS (2007) Expression of prenylated Rab acceptor 1 domain family, member 2 (PRAF2) in neuroblastoma: correlation with clinical features, cellular localization, and cerulenin-mediated apoptosis regulation. Clin Cancer Res **13:** 6312–6319

Geldner N (2004) The plant endosomal system—its structure and role in signal transduction and plant development. Planta **219:** 547–560

Gietz D, St. Jean A, Woods RA, Schiestl RH (1992) Improved method for high efficiency transformation of intact yeast cells. Nucleic Acids Res **20:** 1425

Gilchrist A, Au CE, Hiding J, Bell AW, Fernandez-Rodriguez J, Lesimple S, Nagaya H, Roy L, Gosline SJC, Hallett M, et al (2006) Quantitative proteomics analysis of the secretory pathway. Cell **127:** 1265–1281

Hall TA (1999) BioEdit: a user-friendly biological sequence alignment editor and analysis program for Windows 95/98/NT. Nucleic Acids Symp Ser **41:** 95–98

Hanton SL, Matheson LA, Brandizzi F (2006) Seeking a way out: export of proteins from the plant endoplasmic reticulum. Trends Plant Sci **11:** 335–343

He Z-H, Cheeseman I, He D, Kohorn BD (1999) A cluster of five cell wall-associated receptor kinase genes, *Wak1-5*, are expressed in specific organs of *Arabidopsis*. Plant Mol Biol **39:** 1189–1196

Huang Z, Andrianov VM, Han Y, Howell SH (2001) Identification of Arabidopsis proteins that interact with the cauliflower mosaic virus (CaMV) movement protein. Plant Mol Biol **47:** 663–675

Huh W-K, Falvo JV, Gerke LC, Carroll AS, Howson RW, Weissman JS, O'Shea EK (2003) Global analysis of protein localization in budding yeast. Nature **425:** 686–691

Jallais Y, Fobis-Loisy I, Miège C, Gaude T (2008) Evidence for a sorting endosome in Arabidopsis root cells. Plant J **53:** 237–247

Jürgens G (2004) Membrane trafficking in plants. Annu Rev Cell Dev Biol **20:** 481–504

Karimi M, Bleys A, Vanderhaeghen R, Hilson P (2007) Building blocks for plant gene assembly. Plant Physiol **145:** 1183–1191

Karimi M, Inzé D, Depicker A (2002) GATEWAY™ vectors for *Agrobacterium*-mediated plant transformation. Trends Plant Sci **7:** 193–195

Koizumi K, Naramoto S, Sawa S, Yahara N, Ueda T, Nakano A, Sugiyama M, Fukuda H (2005) VAN3 ARF–GAP-mediated vesicle transport is involved in leaf vascular formation. Development **132:** 1699–1711

Liang Z, Li G (2000) Mouse prenylated Rab acceptor is a novel Golgi membrane protein. Biochem Biophys Res Commun **275:** 509–516

Liang Z, Veeraprame H, Bayan N, Li G (2004) The C-terminus of prenylin is important in forming a dimer conformation necessary for endoplasmic-reticulum-to-Golgi transport. Biochem J **380:** 43–49

Liu H-P, Wu C-C, Chang Y-S (2006) PRA1 promotes the intracellular trafficking and NF-κB signaling of EBV latent membrane protein 1. EMBO J **25:** 4120–4130

Martincic I, Peralta ME, Ngsee JK (1997) Isolation and characterization of a dual prenylated Rab and VAMP2 receptor. J Biol Chem **272:** 26991–26998

Molendijk AJ, Ruperti B, Palme K (2004) Small GTPases in vesicle trafficking. Curr Opin Plant Biol **7:** 694–700

Müller J, Mettbach U, Menzel D, Šamaj J (2007) Molecular dissection of endosomal compartments in plants. Plant Physiol **145:** 293–304

Munro S (1991) Sequences within and adjacent to the transmembrane segment of α-2,6-sialyltransferase specify Golgi retention. EMBO J **10:** 3577–3588

Murashige T, Skoog F (1962) A revised medium for rapid growth and bio assays with tobacco tissue cultures. Physiol Plant **15:** 473–497

Nelson BK, Cai X, Nebenführ A (2007) A multicolored set of *in vivo* organelle markers for co-localization studies in Arabidopsis and other plants. Plant J **51:** 1126–1136

Notredame C, Higgins DG, Heringa J (2000) T-Coffee: a novel method for fast and accurate multiple sequence alignment. J Mol Biol **302:** 205–217

Otte S, Belden WJ, Heidtman M, Liu J, Jensen ON, Barlowe C (2001) Erv41p and Erv46p: new components of COPII vesicles involved in transport between the ER and Golgi complex. J Cell Biol **152:** 503–517

Pfeffer S, Aivazian D (2004) Targeting RAB GTPases to distinct membrane compartments. Nat Rev Mol Cell Biol **5:** 886–896

Reichardt I, Stierhof Y-D, Mayer U, Richter S, Schwarz H, Schumacher K, Jürgens G (2007) Plant cytokinesis requires de novo secretory trafficking but not endocytosis. Curr Biol **17:** 2047–2053

Russinova E, Borst JW, Kwaaitaal M, Caño-Delgado A, Yin Y, Chory J, de Vries SC (2004) Heterodimerization and endocytosis of *Arabidopsis* brassinosteroid receptors BRI1 and AtSERK3 (BAK1). Plant Cell **16:** 3216–3229

Rutherford S, Moore I (2002) The *Arabidopsis* Rab GTPase family: another enigma variation. Curr Opin Plant Biol **5:** 518–528

Saint-Jore-Dupas C, Nebenführ A, Boulaflous A, Follet-Gueye M-L, Plasson C, Hawes C, Driouich A, Faye L, Gomord V (2006) Plant *N*-glycan processing enzymes employ different targeting mechanisms for their spatial arrangement along the secretory pathway. Plant Cell **18:** 3182–3200

Šamaj J, Müller J, Beck M, Böhm N, Menzel D (2006) Vesicular trafficking, cytoskeleton and signalling in root hairs and pollen tubes. Trends Plant Sci **11:** 594–600

Schmidt HA, Strimmer K, Vingron M, von Haeseler A (2002) TREE-PUZZLE: maximum likelihood phylogenetic analysis using quartets and parallel computing. Bioinformatics **18:** 502–504

Schweneker M, Bachmann AS, Moelling K (2005) JM4 is a four-transmembrane protein binding to the CCR5 receptor. FEBS Lett **579:** 1751–1758

Segev N (2001) Ypt/Rab GTPases: regulators of protein trafficking. Sci STKE **100:** re11.1–re11.18

Shope JC, Mott KA (2006) Membrane trafficking and osmotically induced volume changes in guard cells. J Exp Bot **57:** 4123–4131

Sivars U, Aivazian D, Pfeffer SR (2003) Yip3 catalyses the dissociation of endosomal Rab-GDI complexes. Nature **425:** 856–859

Soldati T, Shapiro AD, Svejstrup ABD, Pfeffer SR (1994) Membrane targeting of the small GTPase Rab9 is accompanied by nucleotide exchange. Nature **369:** 76–78

Sutter JU, Campanoni P, Blatt MR, Paneque M (2006) Setting SNAREs in a different wood. Traffic **7:** 627–638

Ullrich O, Horiuchi H, Bucci C, Zerial M (1994) Membrane association of Rab5 mediated by GDP-dissociation inhibitor and accompanied by GDP/GTP exchange. Nature **368:** 157–160

Van de Peer Y, De Wachter R (1993) TREECON: a software package for the construction and drawing of evolutionary trees. Comput Appl Biosci **9:** 177–182

Vandepoele K, Casneuf T, Van de Peer Y (2006). Identification of novel regulatory modules in dicot plants using expression data and comparative genomics. Genome Biol **7:** R103.1–R103.15

Vernoud V, Horton AC, Yang Z, Nielsen E (2003) Analysis of the small GTPase gene superfamily of Arabidopsis. Plant Physiol **131:** 1191–1208